



Observation of the doubly charmed baryon Ξ_{cc}^{++}

LHCb collaboration[†]

Abstract

A highly significant structure is observed in the $\Lambda_c^+ K^- \pi^+ \pi^+$ mass spectrum, where the Λ_c^+ baryon is reconstructed in the decay mode $p K^- \pi^+$. The structure is consistent with originating from a weakly decaying particle, identified as the doubly charmed baryon Ξ_{cc}^{++} . The difference between the masses of the Ξ_{cc}^{++} and Λ_c^+ states is measured to be 1334.94 ± 0.72 (stat) ± 0.27 (syst) MeV/ c^2 , and the Ξ_{cc}^{++} mass is then determined to be 3621.40 ± 0.72 (stat) ± 0.27 (syst) ± 0.14 (Λ_c^+) MeV/ c^2 , where the last uncertainty is due to the limited knowledge of the Λ_c^+ mass. The state is observed in a sample of proton-proton collision data collected by the LHCb experiment at a center-of-mass energy of 13 TeV, corresponding to an integrated luminosity of 1.7 fb^{-1} , and confirmed in an additional sample of data collected at 8 TeV.

Published in Phys. Rev. Lett. 119 (2017) 112001

© CERN on behalf of the LHCb collaboration, license CC-BY-4.0.

[†]Authors are listed at the end of this paper.

The quark model [1–3] predicts the existence of multiplets of baryon and meson states. Those states composed of the lightest four quarks (u, d, s, c) form $SU(4)$ multiplets [4]. Numerous states with charm quantum number $C = 0$ or $C = 1$ have been discovered, including all of the expected $q\bar{q}$ and qqq ground states [5]. Three weakly decaying qqq states with $C = 2$ are expected: one isospin doublet ($\Xi_{cc}^{++} = ccu$ and $\Xi_{cc}^+ = ccd$) and one isospin singlet ($\Omega_{cc}^+ = ccs$), each with spin-parity $J^P = 1/2^+$. The properties of these baryons have been calculated with a variety of theoretical models. In most cases, the masses of the Ξ_{cc} states are predicted to lie in the range 3500 to 3700 MeV/ c^2 [6–33]. The masses of the Ξ_{cc}^{++} and Ξ_{cc}^+ states are expected to differ by only a few MeV/ c^2 , due to approximate isospin symmetry [34–36]. Most predictions for the lifetime of the Ξ_{cc}^+ baryon are in the range 50 to 250 fs, and the lifetime of the Ξ_{cc}^{++} baryon is expected to be three to four times longer at 200 to 700 fs [10, 11, 19, 24, 37–40]. While both are expected to be produced at hadron colliders [41–43], the longer lifetime of the Ξ_{cc}^{++} baryon should make it significantly easier to observe than the Ξ_{cc}^+ baryon in such experiments, due to the use of real-time (online) event-selection requirements designed to reject backgrounds originating from the primary interaction point.

Experimentally, there is a longstanding puzzle in the Ξ_{cc} system. Observations of the Ξ_{cc}^+ baryon at a mass of 3519 ± 2 MeV/ c^2 with signal yields of 15.9 events over 6.1 ± 0.5 background in the final state $\Lambda_c^+ K^- \pi^+$ (6.3σ significance), and 5.62 events over 1.38 ± 0.13 background in the final state $pD^+ K^-$ (4.8σ significance) were reported by the SELEX collaboration [44, 45]. Their results included a number of unexpected features, notably a short lifetime and a large production rate relative to that of the singly charmed Λ_c^+ baryon. The lifetime was stated to be shorter than 33 fs at the 90% confidence level, and SELEX concluded that 20% of all Λ_c^+ baryons observed by the experiment originated from Ξ_{cc}^+ decays, implying a relative Ξ_{cc} production rate several orders of magnitude larger than theoretical expectations [11]. Searches from the FOCUS [46], BaBar [47], and Belle [48] experiments did not find evidence for a state with the properties reported by SELEX, and neither did a search at LHCb with data collected in 2011 corresponding to an integrated luminosity of 0.65 fb^{-1} [49]. However, because the production environments at these experiments differ from that of SELEX, which studied collisions of a hyperon beam on fixed nuclear targets, these null results do not exclude the original observations.

This Letter presents the observation of the Ξ_{cc}^{++} baryon¹ via the decay mode $\Lambda_c^+ K^- \pi^+ \pi^+$ (Fig. 1), which is expected to have a branching fraction of up to 10% [50]. The Λ_c^+ baryon is reconstructed in the final state $pK^- \pi^+$. The data consist of pp collisions collected by the LHCb experiment at the Large Hadron Collider at CERN with a center-of-mass energy of 13 TeV taken in 2016, corresponding to an integrated luminosity of 1.7 fb^{-1} .

The LHCb detector is a single-arm forward spectrometer covering the pseudorapidity range $2 < \eta < 5$, designed for the study of particles containing b or c quarks, and is described in detail in Refs. [51, 52]. The detector elements most relevant to this analysis are a silicon-strip vertex detector surrounding the pp interaction region, a tracking system that provides a measurement of the momentum of charged particles, and two ring-imaging Cherenkov detectors [53] that are able to discriminate between different species of charged hadrons. The online event selection is performed by a trigger that consists of a hardware stage, which is based on information from the calorimeter and muon systems, followed

¹ Inclusion of charge-conjugate processes is implied throughout.

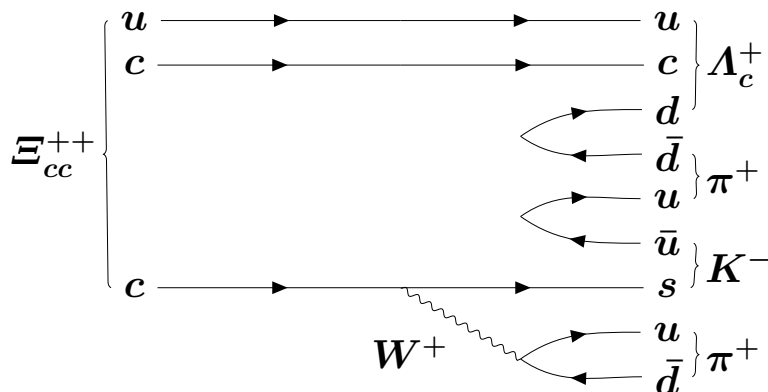


Figure 1: Example Feynman diagram contributing to the decay $\Xi_{cc}^{++} \rightarrow \Lambda_c^+ K^- \pi^+ \pi^+$.

by a software stage, which fully reconstructs the event [54]. The online reconstruction incorporates near-real-time alignment and calibration of the detector [55], which in turn allows the reconstruction of the Ξ_{cc}^{++} decay to be performed entirely in the trigger software.

The reconstruction of $\Xi_{cc}^{++} \rightarrow \Lambda_c^+ K^- \pi^+ \pi^+$ decays proceeds as follows. Candidate $\Lambda_c^+ \rightarrow p K^- \pi^+$ decays are reconstructed from three charged particles that form a good-quality vertex and that are inconsistent with originating from any pp collision primary vertex (PV). The PV of any single particle is defined to be the PV with respect to which the particle has the smallest impact parameter χ^2 (χ_{IP}^2), which is the difference in χ^2 of the PV fit with and without the particle in question. The Λ_c^+ vertex is required to be displaced from its PV by a distance corresponding to a proper decay time greater than 150 fs. The Λ_c^+ candidate is then combined with three additional charged particles to form a $\Xi_{cc}^{++} \rightarrow \Lambda_c^+ K^- \pi^+ \pi^+$ candidate. These additional particles must form a good-quality vertex with the Λ_c^+ candidate, and the Λ_c^+ decay vertex must be downstream of the Ξ_{cc}^{++} vertex. Each of the six final-state particles is required to pass track-quality requirements, to have hadron-identification information consistent with the appropriate hypothesis (p , K , or π), and to have transverse momentum $p_{\text{T}} > 500 \text{ MeV}/c$. To avoid duplicate tracks, the angle between each pair of final-state particles with the same charge is required to be larger than 0.5 mrad. The Ξ_{cc}^{++} candidate must have $p_{\text{T}} > 4 \text{ GeV}/c$ and must be consistent with originating from its PV. The selection above includes criteria applied in the trigger software, plus additional requirements chosen based on simulated signal events and a control sample of data. Simulated signal events are produced with the standard LHCb simulation software [56–62] interfaced to a dedicated generator, GENXICC [63–65], for Ξ_{cc}^{++} baryon production. In the simulation, the Ξ_{cc}^{++} mass and lifetime are assumed to be $3600 \text{ MeV}/c^2$ and 333 fs. The background control sample consists of wrong-sign (WS) $\Lambda_c^+ K^- \pi^+ \pi^-$ combinations.

The background level is further reduced with a multivariate selector based on the multilayer perceptron algorithm [66]. The selector is trained with simulated signal events and with the WS control sample of data to represent the background. For both signal and background training samples, candidates are required to pass the selection described above and to fall within a signal search region defined as $2270 < m_{\text{cand}}(\Lambda_c^+) < 2306 \text{ MeV}/c^2$ and

$3300 < m_{\text{cand}}(\Xi_{cc}^{++}) < 3800 \text{ MeV}/c^2$, where $m_{\text{cand}}(\Lambda_c^+)$ is the reconstructed mass of the Λ_c^+ candidate, $m_{\text{cand}}(\Xi_{cc}^{++}) \equiv m(\Lambda_c^+ K^- \pi^+ \pi^\pm) - m_{\text{cand}}(\Lambda_c^+) + m_{\text{PDG}}(\Lambda_c^+)$, $m(\Lambda_c^+ K^- \pi^+ \pi^\pm)$ is the reconstructed mass of the $\Lambda_c^+ K^- \pi^+ \pi^\pm$ combination, and $m_{\text{PDG}}(\Lambda_c^+) = 2286.46 \pm 0.14 \text{ MeV}/c^2$ is the known value of the Λ_c^+ mass [5]. The $m_{\text{cand}}(\Lambda_c^+)$ window corresponds to approximately ± 3 times the Λ_c^+ mass resolution. The use of $m_{\text{cand}}(\Xi_{cc}^{++})$ rather than $m(\Lambda_c^+ K^- \pi^+ \pi^\pm)$ cancels fluctuations in the reconstructed Λ_c^+ mass to first order, and thereby improves the Ξ_{cc}^{++} mass resolution by approximately 40%.

Based on studies with simulated events and control samples of data, ten input variables that together provide good discrimination between signal and background candidates are used in the multivariate selector. They are as follows: the χ^2 per degree of freedom of each of the Λ_c^+ vertex fit, the Ξ_{cc}^{++} vertex fit, and a kinematic refit [67] of the Ξ_{cc}^{++} decay chain requiring it to originate from its PV; the smallest p_T of the three decay products of the Λ_c^+ ; the smallest p_T of the four decay products of the Ξ_{cc}^{++} ; the scalar sum of the p_T of the four decay products of the Ξ_{cc}^{++} ; the angle between the Ξ_{cc}^{++} momentum vector and the direction from the PV to the Ξ_{cc}^{++} decay vertex; the flight distance χ^2 between the PV and the Ξ_{cc}^{++} decay vertex; the χ_{IP}^2 of the Ξ_{cc}^{++} with respect to its PV; and the smallest χ_{IP}^2 of the decay products of the Ξ_{cc}^{++} with respect to its PV. Here, the flight distance χ^2 is defined as the χ^2 of the hypothesis that the Ξ_{cc}^{++} decay vertex coincides with its PV. Candidates are retained for analysis only if their multivariate selector output values exceed a threshold chosen by maximizing the expected value of the figure of merit $\varepsilon/(\frac{5}{2} + \sqrt{B})$ [68], where ε is the estimated signal efficiency and B is the estimated number of background candidates underneath the signal peak. The quantity B is computed with the WS control sample and, purely for the purposes of this optimization, it is calculated in a window centered at a mass of $3600 \text{ MeV}/c^2$ and of halfwidth $12.5 \text{ MeV}/c^2$ (corresponding to approximately twice the expected resolution). Its evaluation takes into account the difference in background rates between the $\Lambda_c^+ K^- \pi^+ \pi^\pm$ signal mode and the WS sample, scaling the WS background by the ratio seen in data in the sideband regions $3200 < m_{\text{cand}}(\Xi_{cc}^{++}) < 3300 \text{ MeV}/c^2$ and $3800 < m_{\text{cand}}(\Xi_{cc}^{++}) < 3900 \text{ MeV}/c^2$. The performance of the multivariate selector is also tested for simulated signal events under other lifetime hypotheses; while the signal efficiency increases with the lifetime, it is found that the training obtained for 333 fs is close to optimal (*i.e.* gives comparable performance to a training optimized for the new lifetime hypothesis) even for much shorter or longer lifetimes.

After the multivariate selection is applied, events may still contain more than one Ξ_{cc}^{++} candidate in the signal search region. Based on studies of simulation and the control data sample, no peaking background arises due to multiple candidates except for the special case in which the candidates are formed from the same six decay products but two of the decay products are interchanged (*e.g.*, the K^- particle from the Ξ_{cc}^{++} decay and the K^- particle from the Λ_c^+ decay). In such instances, one of the candidates is chosen at random to be retained and all others are discarded. In the remaining events, the fraction that has more than one Ξ_{cc}^{++} candidate in the range $3300\text{--}3800 \text{ MeV}/c^2$ is approximately 8%.

The selection described above is then applied to data in the search region. Figure 2 shows the Λ_c^+ mass distribution, and the Ξ_{cc}^{++} mass spectra for candidates in the mass range $2270 < m_{\text{cand}}(\Lambda_c^+) < 2306 \text{ MeV}/c^2$. A structure is visible in the signal mode at a mass of approximately $3620 \text{ MeV}/c^2$. No significant structure is visible in the WS control sample, nor for events in the Λ_c^+ mass sidebands. To measure the properties of the structure, an unbinned extended maximum likelihood fit is performed to the invariant mass distribution in the restricted $\Lambda_c^+ K^- \pi^+ \pi^\pm$ mass window of $3620 \pm 150 \text{ MeV}/c^2$ (Fig. 3).

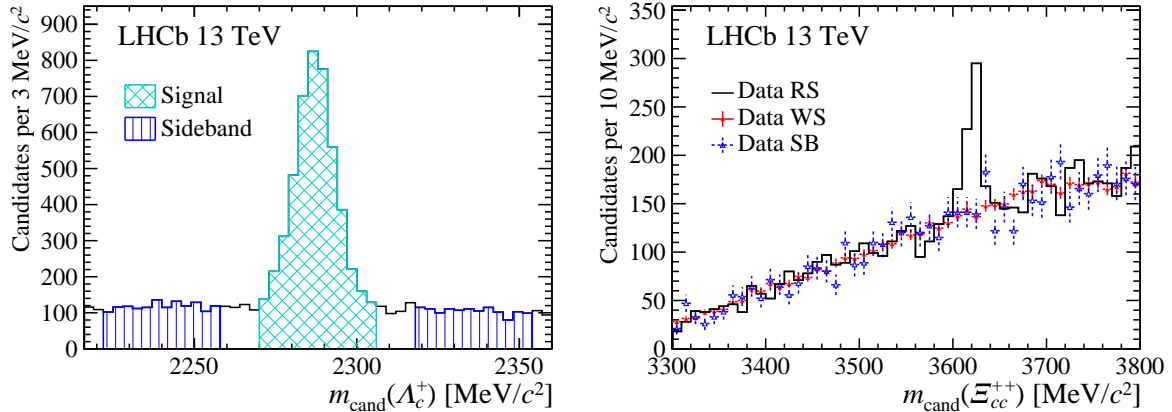


Figure 2: Mass spectra of (left) Λ_c^+ and (right) Ξ_{cc}^{++} candidates. The full selection is applied, except for the Λ_c^+ mass requirement in the case of the left plot. For the Λ_c^+ mass distribution the (cross-hatched) signal and (vertical line) sideband regions are indicated; to avoid duplication, the histogram is filled only once in events that contain more than one Ξ_{cc}^{++} candidate. In the right plot the right-sign (RS) signal sample $\Xi_{cc}^{++} \rightarrow \Lambda_c^+ K^- \pi^+ \pi^+$ is shown, along with the control samples: Λ_c^+ sideband (SB) $\Lambda_c^+ K^- \pi^+ \pi^+$ candidates and wrong-sign (WS) $\Lambda_c^+ K^- \pi^+ \pi^-$ candidates, normalized to have the same area as the RS sample in the $m_{\text{cand}}(\Xi_{cc}^{++})$ sidebands.

The peaking structure is empirically described by a Gaussian function plus a modified Gaussian function with power-law tails on both sides [69]. All peak parameters are fixed to values obtained from simulation apart from the mass, yield, and an overall resolution parameter. The background is described by a second-order polynomial with parameters free to float in the fit. The signal yield is measured to be 313 ± 33 , corresponding to a local statistical significance in excess of 12σ when evaluated with a likelihood ratio test. The fitted resolution parameter is $6.6 \pm 0.8 \text{ MeV}/c^2$, consistent with simulation. The same structure is also observed in the $\Lambda_c^+ K^- \pi^+ \pi^+$ spectrum in a pp data sample collected by LHCb at $\sqrt{s} = 8 \text{ TeV}$ (see supplemental material in Appendix A for results from the 8 TeV cross-check sample). The local statistical significance of the peak in the 8 TeV sample is above 7σ , and its mass is consistent with that in the 13 TeV data sample.

Additional cross-checks are performed confirming the robustness of the observation. The significance of the structure in the $\Lambda_c^+ K^- \pi^+ \pi^+$ final state remains above 12σ when fixing the resolution parameter in the invariant mass fit to the value obtained from simulation, changing the threshold value for the multivariate selector, removing events containing multiple candidates in the fitted mass range, or using an alternative selection without a multivariate classifier. The significance also remains above 12σ in a subsample of candidates for which the reconstructed decay time exceeds five times its uncertainty. This is consistent with a weakly decaying state and inconsistent with the strong decay of a resonance. No fake peaking structures are observed in the control samples when requiring various intermediate resonances to be present (ρ^0 , K^{*0} , Σ_c^0 , Σ_c^{++} , Λ_c^{*+}) nor are they observed when combining Ξ_{cc}^{++} and Λ_c^+ decay products. The contributions of misidentified $D_s^+ \rightarrow K^+ K^- \pi^+$ and $D^+ \rightarrow K^- \pi^+ \pi^+$ decays are found to be negligible.

The sources of systematic uncertainty affecting the measurement of the Ξ_{cc}^{++} mass (Table 1) include the momentum-scale calibration, the event selection, the unknown Ξ_{cc}^{++} lifetime, the invariant mass fit model, and the uncertainty on the Λ_c^+ mass. The momentum

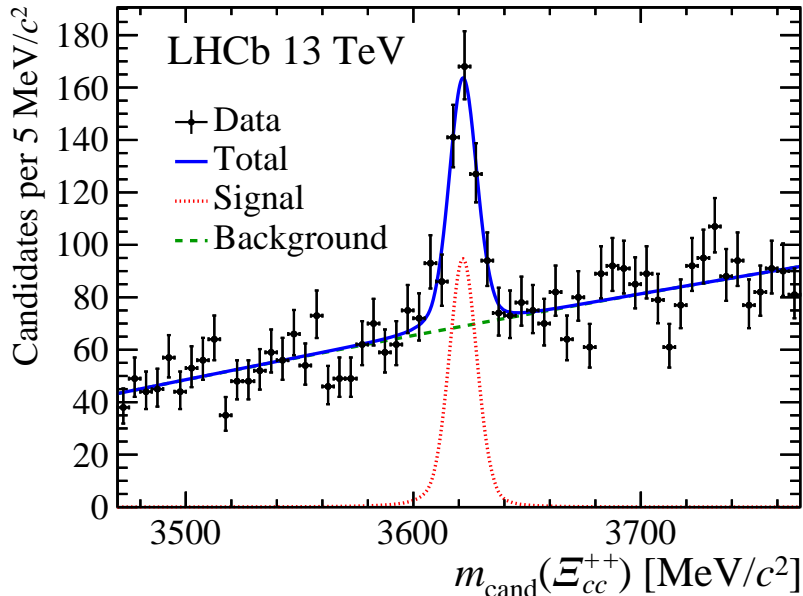


Figure 3: Invariant mass distribution of $\Lambda_c^+ K^- \pi^+ \pi^+$ candidates with fit projections overlaid.

scale is calibrated with samples of $J/\psi \rightarrow \mu^+ \mu^-$ and $B^+ \rightarrow J/\psi K^+$ decays [70, 71]. After calibration, an uncertainty of $\pm 0.03\%$ is assigned, which corresponds to a systematic uncertainty of $0.22 \text{ MeV}/c^2$ on the reconstructed Ξ_{cc}^{++} mass. The selection procedure is more efficient for vertices that are well separated from the PV, and therefore preferentially retains longer-lived Ξ_{cc}^{++} candidates. Because of a correlation between the reconstructed decay time and the reconstructed mass, this induces a positive bias on the mass for both Ξ_{cc}^{++} and Λ_c^+ candidates. The effect is studied with simulation and the bias on the Ξ_{cc}^{++} mass is determined to be $+0.45 \pm 0.14 \text{ MeV}/c^2$ (assuming a lifetime of 333 fs), where the uncertainty is due to the limited size of the simulation sample. A corresponding correction is applied to the fitted value in data. To validate this procedure, the Λ_c^+ mass in an inclusive sample is measured and corrected in the same way; after the correction, the Λ_c^+ mass is found to agree with the known value [5]. The bias on the Ξ_{cc}^{++} mass depends on the unknown Ξ_{cc}^{++} lifetime, introducing a further source of uncertainty on the correction. This is estimated by repeating the procedure for other Ξ_{cc}^{++} lifetime hypotheses between 200 and 700 fs. The largest deviation in the correction, $0.06 \text{ MeV}/c^2$, is taken as an additional systematic uncertainty. Final-state photon radiation also causes a bias in the measured mass, which is determined to be $-0.05 \text{ MeV}/c^2$ with simulation [60]. The uncertainty on this correction is approximately $0.01 \text{ MeV}/c^2$ and is neglected. The dependence of the measurement on the fit model is estimated by varying the shape parameters that are fixed according to simulation, by using alternative signal and background models, and by repeating the fits in different mass ranges. The largest deviation seen in the mass, $0.07 \text{ MeV}/c^2$, is assigned as a systematic uncertainty. Finally, since the Ξ_{cc}^{++} mass is measured relative to the Λ_c^+ mass, the uncertainty of $0.14 \text{ MeV}/c^2$ on the world-average value of the latter is included. After taking these systematic effects into account and combining their uncertainties (except that on the Λ_c^+ mass) in quadrature, the Ξ_{cc}^{++} mass is measured to be $3621.40 \pm 0.72 \text{ (stat)} \pm 0.27 \text{ (syst)} \pm 0.14 \text{ (}\Lambda_c^+\text{)} \text{ MeV}/c^2$. The mass

Table 1: Systematic uncertainties on the Ξ_{cc}^{++} mass measurement.

Source	Value [MeV/ c^2]
Momentum-scale calibration	0.22
Selection bias correction	0.14
Unknown Ξ_{cc}^{++} lifetime	0.06
Mass fit model	0.07
Sum of above in quadrature	0.27
Λ_c^+ mass uncertainty	0.14

difference between the Ξ_{cc}^{++} and Λ_c^+ states is 1334.94 ± 0.72 (stat) ± 0.27 (syst) MeV/ c^2 .

In summary, a highly significant structure is observed in the final state $\Lambda_c^+ K^- \pi^+ \pi^+$ in a pp data sample collected by LHCb at $\sqrt{s} = 13$ TeV, with a signal yield of 313 ± 33 . The mass of the structure is measured to be 3621.40 ± 0.72 (stat) ± 0.27 (syst) ± 0.14 (Λ_c^+) MeV/ c^2 , where the last uncertainty is due to the limited knowledge of the Λ_c^+ mass, and its width is consistent with experimental resolution. The structure is confirmed with consistent mass in a data set collected by LHCb at $\sqrt{s} = 8$ TeV. The signal candidates have significant decay lengths, and the signal remains highly significant after a minimum lifetime requirement of approximately five times the expected decay-time resolution is imposed. This state is therefore incompatible with a strongly decaying particle but is consistent with the expectations for the weakly decaying Ξ_{cc}^{++} baryon. The mass of the observed Ξ_{cc}^{++} state is greater than that of the Ξ_{cc}^+ peaks reported by the SELEX collaboration [44, 45] by 103 ± 2 MeV/ c^2 . This difference would imply an isospin splitting vastly larger than that seen in any other baryon system and is inconsistent with the expected size of a few MeV/ c^2 [34–36]. Consequently, while the state reported here is consistent with most theoretical expectations for the Ξ_{cc}^{++} baryon, it is inconsistent with being an isospin partner to the Ξ_{cc}^+ state reported previously by the SELEX collaboration.

Acknowledgements

We thank Chao-Hsi Chang, Cai-Dian Lü, Xing-Gang Wu, and Fu-Sheng Yu for frequent and interesting discussions on the production and decays of double-heavy-flavor baryons. We express our gratitude to our colleagues in the CERN accelerator departments for the excellent performance of the LHC. We thank the technical and administrative staff at the LHCb institutes. We acknowledge support from CERN and from the national agencies: CAPES, CNPq, FAPERJ and FINEP (Brazil); MOST and NSFC (China); CNRS/IN2P3 (France); BMBF, DFG and MPG (Germany); INFN (Italy); NWO (The Netherlands); MNiSW and NCN (Poland); MEN/IFA (Romania); MinES and FASO (Russia); MinECo (Spain); SNSF and SER (Switzerland); NASU (Ukraine); STFC (United Kingdom); NSF (USA). We acknowledge the computing resources that are provided by CERN, IN2P3 (France), KIT and DESY (Germany), INFN (Italy), SURF (The Netherlands), PIC (Spain), GridPP (United Kingdom), RRCKI and Yandex LLC (Russia), CSCS (Switzerland), IFIN-HH (Romania), CBPF (Brazil), PL-GRID (Poland) and OSC (USA). We are indebted to the communities behind the multiple open source software packages on which we depend. Individual groups or members have received support from AvH Foundation (Germany), EPLANET, Marie Skłodowska-Curie Actions and ERC (European Union), Conseil Général

de Haute-Savoie, Labex ENIGMASS and OCEVU, Région Auvergne (France), RFBR and Yandex LLC (Russia), GVA, XuntaGal and GENCAT (Spain), Herchel Smith Fund, The Royal Society, Royal Commission for the Exhibition of 1851 and the Leverhulme Trust (United Kingdom).

A Appendix: Supplemental material

The Letter describes the observation of a narrow structure in the $\Lambda_c^+ K^- \pi^+ \pi^+$ mass spectrum in a sample of data collected by the LHCb experiment in 2016 at a center-of-mass energy of 13 TeV, corresponding to an integrated luminosity of 1.7 fb^{-1} . In addition, as a cross-check, a similar study is carried out on a separate data sample collected in 2012 at a center-of-mass energy of 8 TeV, corresponding to an integrated luminosity of 2.0 fb^{-1} . The 13 TeV sample has greater sensitivity, due both to an increase in the expected cross-section at higher center-of-mass energy and to improvements in the online selection between the data-taking periods. Nonetheless, a smaller but still highly significant signal is also found in the 8 TeV sample, with properties fully compatible with those of the signal seen in the 13 TeV sample. This serves as a useful, and statistically independent, validation. In this supplemental material, the differences between the two data samples are outlined and results from the cross-check 8 TeV sample are shown.

Data taken during 2012 follow an event processing model in which events are first required to pass a multi-level online event selection. The online selection used for this study is the same as that described in Ref. [49]. The events are then analyzed offline and the decay chain $\Xi_{cc}^{++} \rightarrow \Lambda_c^+ K^- \pi^+ \pi^+$ is reconstructed following the procedure described in the Letter. The Ξ_{cc}^{++} candidates are required to pass the same series of selection criteria as for the 13 TeV sample, as well as three additional requirements (on the p_T of the products of the Λ_c^+ decay, on the particle identification information of the π^+ from the Λ_c^+ decay, and on the distances of closest approach of the decay products of the Ξ_{cc}^{++} to one another) that were applied as part of an initial event filtering pass. Candidates are also required to pass the multivariate selector described in the Letter. For consistency, the same selector used in the 13 TeV sample was applied to the 8 TeV sample. However, the threshold on the selector output was reoptimized with control samples with a center-of-mass energy of 8 TeV.

Figure 4 shows the Λ_c^+ and Ξ_{cc}^{++} mass spectra in the 8 TeV sample after the final selection. As with the 13 TeV sample, a narrow structure is visible in the signal mode but no structure is seen in the control samples. The fit procedure described in the Letter is applied to the 8 TeV right-sign sample, and the results are shown in Fig. 5. The signal yield is measured to be 113 ± 21 , and corresponds to a statistical significance in excess of seven standard deviations. The fitted mass differs from that in the 13 TeV sample by $0.8 \pm 1.4 \text{ MeV}/c^2$ (where the uncertainty is statistical only). The fitted resolution parameter is $6.6 \pm 1.4 \text{ MeV}/c^2$, consistent with that in the 13 TeV sample and with the value expected from simulation. The resolution parameter is the weighted average of the widths of the two Gaussian functions of the signal mass fit model. Thus, the fitted properties of the structures seen in the two samples are consistent, and we conclude that they are associated with the same physical process. Combined with the yield of 313 ± 33 in the 13 TeV data sample, the total signal yield in the two samples is 426 ± 39 .

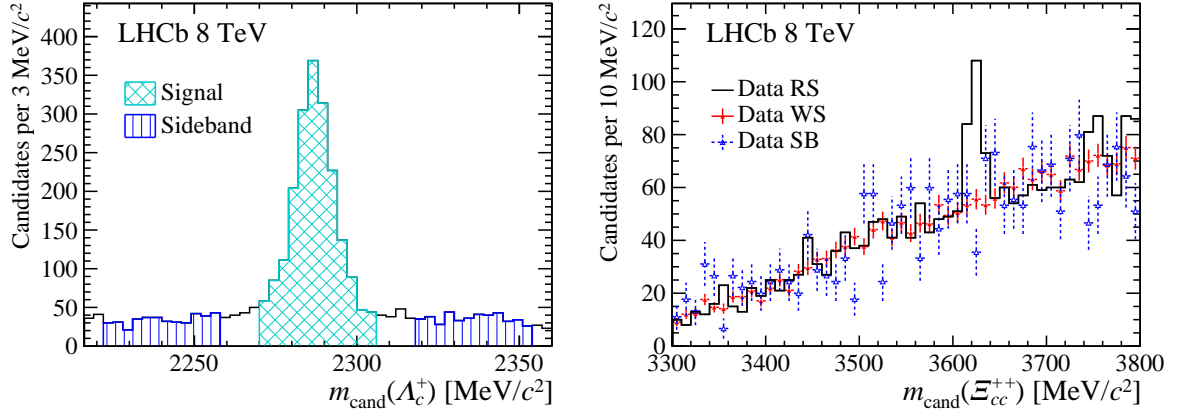


Figure 4: Mass spectra of (left) Λ_c^+ and (right) Ξ_{cc}^{++} candidates in the 8 TeV data sample. The full selection is applied, except for the Λ_c^+ mass requirement in the case of the left plot. For the Λ_c^+ mass distribution the (cross-hatched) signal and (vertical lines) sideband regions are indicated; to avoid duplication, the histogram is filled only once in events that contain more than one Ξ_{cc}^{++} candidate. In the right plot the right-sign (RS) signal sample $\Xi_{cc}^{++} \rightarrow \Lambda_c^+ K^- \pi^+ \pi^+$ is shown, along with the control samples: Λ_c^+ sideband (SB) $\Lambda_c^+ K^- \pi^+ \pi^+$ candidates and wrong-sign (WS) $\Lambda_c^+ K^- \pi^+ \pi^-$ candidates, normalized to have the same area as the RS sample in the $m_{\text{cand}}(\Xi_{cc}^{++})$ sidebands.

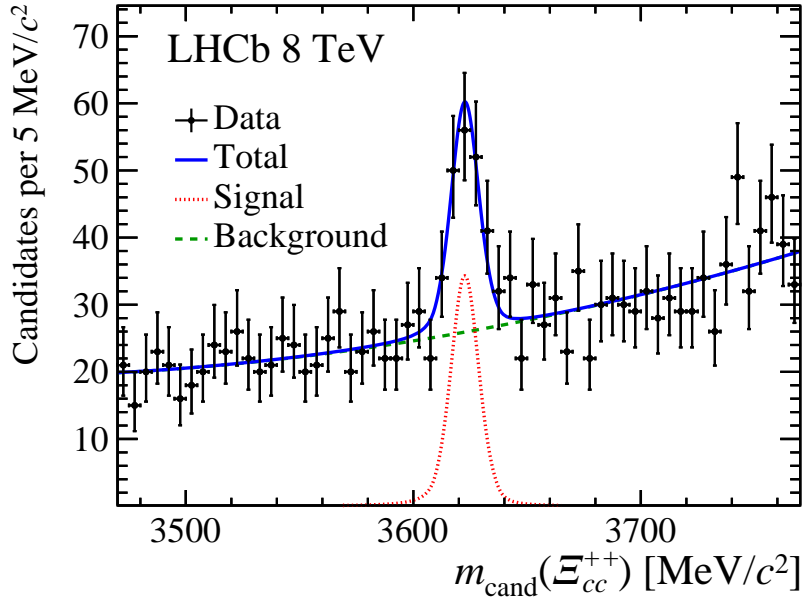


Figure 5: Invariant mass distribution of $\Lambda_c^+ K^- \pi^+ \pi^+$ candidates for the 8 TeV data sample with fit projections overlaid.

References

- [1] M. Gell-Mann, *A schematic model of baryons and mesons*, Phys. Lett. **8** (1964) 214.
- [2] G. Zweig, *An $SU(3)$ model for strong interaction symmetry and its breaking, Part 1*, 1964. CERN-TH-401.
- [3] G. Zweig, *An $SU(3)$ model for strong interaction symmetry and its breaking, Part 2*, 1964. CERN-TH-412, Published in ‘Developments in the Quark Theory of Hadrons’. Volume 1. Edited by D. Lichtenberg and S. Rosen. Nonantum, Mass., Hadronic Press, 1980. pp. 22–101.
- [4] A. De Rújula, H. Georgi, and S. L. Glashow, *Hadron masses in a gauge theory*, Phys. Rev. **D12** (1975) 147.
- [5] Particle Data Group, C. Patrignani *et al.*, *Review of particle physics*, Chin. Phys. **C40** (2016) 100001, and 2017 update.
- [6] S. S. Gershtein, V. V. Kiselev, A. K. Likhoded, and A. I. Onishchenko, *Spectroscopy of doubly heavy baryons*, Phys. Atom. Nucl. **63** (2000) 274, arXiv:hep-ph/9811212, [Yad. Fiz. 63, 334 (2000)].
- [7] S. S. Gershtein, V. V. Kiselev, A. K. Likhoded, and A. I. Onishchenko, *Spectroscopy of doubly charmed baryons: Ξ_{cc}^+ and Ξ_{cc}^{++}* , Mod. Phys. Lett. **A14** (1999) 135, arXiv:hep-ph/9807375.
- [8] C. Itoh, T. Minamikawa, K. Miura, and T. Watanabe, *Doubly charmed baryon masses and quark wave functions in baryons*, Phys. Rev. **D61** (2000) 057502.
- [9] S. S. Gershtein, V. V. Kiselev, A. K. Likhoded, and A. I. Onishchenko, *Spectroscopy of doubly heavy baryons*, Phys. Rev. **D62** (2000) 054021.
- [10] K. Anikeev *et al.*, *B physics at the Tevatron: Run II and beyond*, in *Workshop on B physics at the Tevatron: Run II and beyond, Batavia, Illinois, September 23-25, 1999*, 2001. arXiv:hep-ph/0201071.
- [11] V. V. Kiselev and A. K. Likhoded, *Baryons with two heavy quarks*, Phys. Usp. **45** (2002) 455, arXiv:hep-ph/0103169.
- [12] D. Ebert, R. N. Faustov, V. O. Galkin, and A. P. Martynenko, *Mass spectra of doubly heavy baryons in the relativistic quark model*, Phys. Rev. **D66** (2002) 014008, arXiv:hep-ph/0201217.
- [13] D.-H. He *et al.*, *Evaluation of the spectra of baryons containing two heavy quarks in a bag model*, Phys. Rev. **D70** (2004) 094004, arXiv:hep-ph/0403301.
- [14] C.-H. Chang, C.-F. Qiao, J.-X. Wang, and X.-G. Wu, *Estimate of the hadronic production of the doubly charmed baryon Ξ_{cc} in the general-mass variable-flavor-number scheme*, Phys. Rev. **D73** (2006) 094022, arXiv:hep-ph/0601032.
- [15] W. Roberts and M. Pervin, *Heavy baryons in a quark model*, Int. J. Mod. Phys. **A23** (2008) 2817, arXiv:0711.2492.

- [16] A. Valcarce, H. Garcilazo, and J. Vijande, *Towards an understanding of heavy baryon spectroscopy*, Eur. Phys. J. **A37** (2008) 217, arXiv:0807.2973.
- [17] J.-R. Zhang and M.-Q. Huang, *Doubly heavy baryons in QCD sum rules*, Phys. Rev. **D78** (2008) 094007, arXiv:0810.5396.
- [18] Z.-G. Wang, *Analysis of the $\frac{1}{2}^+$ doubly heavy baryon states with QCD sum rules*, Eur. Phys. J. **A45** (2010) 267, arXiv:1001.4693.
- [19] M. Karliner and J. L. Rosner, *Baryons with two heavy quarks: masses, production, decays, and detection*, Phys. Rev. **D90** (2014) 094007, arXiv:1408.5877.
- [20] K.-W. Wei, B. Chen, and X.-H. Guo, *Masses of doubly and triply charmed baryons*, Phys. Rev. **D92** (2015) 076008, arXiv:1503.05184.
- [21] Z.-F. Sun and M. J. Vicente Vacas, *Masses of doubly charmed baryons in the extended on-mass-shell renormalization scheme*, Phys. Rev. **D93** (2016) 094002, arXiv:1602.04714.
- [22] C. Alexandrou and C. Kallidonis, *Low-lying baryon masses using $N_f = 2$ twisted mass clover-improved fermions directly at the physical pion mass*, Phys. Rev. **D96** (2017) 034511, arXiv:1704.02647.
- [23] B. O. Kerbikov, M. I. Polikarpov, and L. V. Shevchenko, *Multiquark masses and wave functions through a modified Green function Monte Carlo method*, Nucl. Phys. **B331** (1990) 19.
- [24] S. Fleck and J.-M. Richard, *Baryons with double charm*, Prog. Theor. Phys. **82** (1989) 760.
- [25] S. Chernyshev, M. A. Nowak, and I. Zahed, *Heavy hadrons and QCD instantons*, Phys. Rev. **D53** (1996) 5176, arXiv:hep-ph/9510326.
- [26] T. M. Aliev, K. Azizi, and M. Savcı, *Doubly heavy spin-1/2 baryon spectrum in QCD*, Nucl. Phys. **A895** (2012) 59, arXiv:1205.2873.
- [27] Z.-F. Sun, Z.-W. Liu, X. Liu, and S.-L. Zhu, *Masses and axial currents of the doubly charmed baryons*, Phys. Rev. **D91** (2015) 094030, arXiv:1411.2117.
- [28] N. Mathur, R. Lewis, and R. M. Woloshyn, *Charmed and bottom baryons from lattice nonrelativistic QCD*, Phys. Rev. **D66** (2002) 014502, arXiv:hep-ph/0203253.
- [29] PACS-CS collaboration, Y. Namekawa *et al.*, *Charmed baryons at the physical point in 2+1 flavor lattice QCD*, Phys. Rev. **D87** (2013) 094512, arXiv:1301.4743.
- [30] Z. S. Brown, W. Detmold, S. Meinel, and K. Orginos, *Charmed bottom baryon spectroscopy from lattice QCD*, Phys. Rev. **D90** (2014) 094507, arXiv:1409.0497.
- [31] M. Padmanath, R. G. Edwards, N. Mathur, and M. Peardon, *Spectroscopy of doubly charmed baryons from lattice QCD*, Phys. Rev. **D91** (2015) 094502, arXiv:1502.01845.

- [32] P. Pérez-Rubio, S. Collins, and G. S. Bali, *Charmed baryon spectroscopy and light flavor symmetry from lattice QCD*, Phys. Rev. **D92** (2015) 034504, arXiv:1503.08440.
- [33] Y. Liu and I. Zahed, *Heavy baryons and their exotics from instantons in holographic QCD*, Phys. Rev. **D95** (2017) 116012, arXiv:1704.03412; Y. Liu and I. Zahed, *Heavy and strange holographic baryons*, arXiv:1705.01397.
- [34] C.-W. Hwang and C.-H. Chung, *Isospin mass splittings of heavy baryons in heavy quark symmetry*, Phys. Rev. **D78** (2008) 073013, arXiv:0804.4044.
- [35] S. J. Brodsky, F.-K. Guo, C. Hanhart, and U.-G. Meißner, *Isospin splittings of doubly heavy baryons*, Phys. Lett. **B698** (2011) 251, arXiv:1101.1983.
- [36] M. Karliner and J. L. Rosner, *Isospin splittings in baryons with two heavy quarks*, Phys. Rev. **D96** (2017) 033004, arXiv:1706.06961.
- [37] B. Guberina, B. Melić, and H. Štefančić, *Inclusive decays and lifetimes of doubly charmed baryons*, Eur. Phys. J. **C9** (1999) 213, Erratum ibid. **C13** (2000) 551, arXiv:hep-ph/9901323.
- [38] V. V. Kiselev, A. K. Likhoded, and A. I. Onishchenko, *Lifetimes of doubly charmed baryons: Ξ_{cc}^+ and Ξ_{cc}^{++}* , Phys. Rev. **D60** (1999) 014007, arXiv:hep-ph/9807354.
- [39] C.-H. Chang, T. Li, X.-Q. Li, and Y.-M. Wang, *Lifetime of doubly charmed baryons*, Commun. Theor. Phys. **49** (2008) 993, arXiv:0704.0016.
- [40] A. V. Berezhnoy and A. K. Likhoded, *Doubly heavy baryons*, Phys. Atom. Nucl. **79** (2016) 260, [Yad. Fiz. 79, 151 (2016)].
- [41] A. V. Berezhnoy, A. K. Likhoded, and M. V. Shevlyagin, *Hadronic production of B_c^+ mesons*, Phys. Atom. Nucl. **58** (1995) 672, arXiv:hep-ph/9408284, [Yad. Fiz. 58, 730 (1995)].
- [42] K. Kolodziej, A. Leike, and R. Ruckl, *Production of B_c^+ mesons in hadronic collisions*, Phys. Lett. **B355** (1995) 337, arXiv:hep-ph/9505298.
- [43] A. V. Berezhnoy, V. V. Kiselev, A. K. Likhoded, and A. I. Onishchenko, *Doubly charmed baryon production in hadronic experiments*, Phys. Rev. **D57** (1998) 4385, arXiv:hep-ph/9710339.
- [44] SELEX collaboration, M. Mattson *et al.*, *First observation of the doubly charmed baryon Ξ_{cc}^+* , Phys. Rev. Lett. **89** (2002) 112001, arXiv:hep-ex/0208014.
- [45] SELEX collaboration, A. Ocherashvili *et al.*, *Confirmation of the double charm baryon $\Xi_{cc}^+(3520)$ via its decay to pD^+K^-* , Phys. Lett. **B628** (2005) 18, arXiv:hep-ex/0406033.
- [46] S. P. Ratti, *New results on c -baryons and a search for cc -baryons in FOCUS*, Nucl. Phys. Proc. Suppl. **115** (2003) 33.
- [47] BaBar collaboration, B. Aubert *et al.*, *Search for doubly charmed baryons Ξ_{cc}^+ and Ξ_{cc}^{++} in BABAR*, Phys. Rev. **D74** (2006) 011103, arXiv:hep-ex/0605075.

- [48] Belle collaboration, R. Chistov *et al.*, *Observation of new states decaying into $\Lambda_c^+ K^- \pi^+$ and $\Lambda_c^+ K_s^0 \pi^-$* , Phys. Rev. Lett. **97** (2006) 162001, [arXiv:hep-ex/0606051](#).
- [49] LHCb collaboration, R. Aaij *et al.*, *Search for the doubly charmed baryon Ξ_{cc}^+* , JHEP **12** (2013) 090, [arXiv:1310.2538](#).
- [50] F.-S. Yu *et al.*, *Discovery potentials of doubly charmed baryons*, [arXiv:1703.09086](#).
- [51] LHCb collaboration, A. A. Alves Jr. *et al.*, *The LHCb detector at the LHC*, JINST **3** (2008) S08005.
- [52] LHCb collaboration, R. Aaij *et al.*, *LHCb detector performance*, Int. J. Mod. Phys. **A30** (2015) 1530022, [arXiv:1412.6352](#).
- [53] M. Adinolfi *et al.*, *Performance of the LHCb RICH detector at the LHC*, Eur. Phys. J. **C73** (2013) 2431, [arXiv:1211.6759](#).
- [54] R. Aaij *et al.*, *The LHCb trigger and its performance in 2011*, JINST **8** (2013) P04022, [arXiv:1211.3055](#).
- [55] G. Dujany and B. Storaci, *Real-time alignment and calibration of the LHCb detector in Run II*, J. Phys. Conf. Ser. **664** (2015) 082010.
- [56] T. Sjöstrand, S. Mrenna, and P. Skands, *A brief introduction to PYTHIA 8.1*, Comput. Phys. Commun. **178** (2008) 852, [arXiv:0710.3820](#).
- [57] T. Sjöstrand, S. Mrenna, and P. Skands, *PYTHIA 6.4 physics and manual*, JHEP **05** (2006) 026, [arXiv:hep-ph/0603175](#).
- [58] I. Belyaev *et al.*, *Handling of the generation of primary events in Gauss, the LHCb simulation framework*, J. Phys. Conf. Ser. **331** (2011) 032047.
- [59] D. J. Lange, *The EvtGen particle decay simulation package*, Nucl. Instrum. Meth. **A462** (2001) 152.
- [60] P. Golonka and Z. Was, *PHOTOS Monte Carlo: a precision tool for QED corrections in Z and W decays*, Eur. Phys. J. **C45** (2006) 97, [arXiv:hep-ph/0506026](#).
- [61] Geant4 collaboration, S. Agostinelli *et al.*, *Geant4: a simulation toolkit*, Nucl. Instrum. Meth. **A506** (2003) 250; Geant4 collaboration, J. Allison *et al.*, *Geant4 developments and applications*, IEEE Trans. Nucl. Sci. **53** (2006) 270.
- [62] M. Clemencic *et al.*, *The LHCb simulation application, Gauss: design, evolution and experience*, J. Phys. Conf. Ser. **331** (2011) 032023.
- [63] C.-H. Chang, J.-X. Wang, and X.-G. Wu, *GENXICC: a generator for hadronic production of the double heavy baryons Ξ_{cc} , Ξ_{bc} and Ξ_{bb}* , Comput. Phys. Commun. **177** (2007) 467, [arXiv:hep-ph/0702054](#).
- [64] C.-H. Chang, J.-X. Wang, and X.-G. Wu, *GENXICC2.0: an upgraded version of the generator for hadronic production of double heavy baryons Ξ_{cc} , Ξ_{bc} and Ξ_{bb}* , Comput. Phys. Commun. **181** (2010) 1144, [arXiv:0910.4462](#).

- [65] X.-Y. Wang and X.-G. Wu, *GENXICC2.1: an improved version of GENXICC for hadronic production of doubly heavy baryons*, Comput. Phys. Commun. **184** (2013) 1070, arXiv:1210.3458.
- [66] A. Hoecker *et al.*, *TMVA: the Toolkit for Multivariate Data Analysis with ROOT*, PoS **ACAT** (2007) 040, arXiv:physics/0703039.
- [67] W. D. Hulsbergen, *Decay chain fitting with a Kalman filter*, Nucl. Instrum. Meth. **A552** (2005) 566, arXiv:physics/0503191.
- [68] G. Punzi, *Sensitivity of searches for new signals and its optimization*, in *Statistical Problems in Particle Physics, Astrophysics, and Cosmology* (L. Lyons, R. Mount, and R. Reitmeyer, eds.), p. 79, 2003. arXiv:physics/0308063.
- [69] T. Skwarnicki, *A study of the radiative cascade transitions between the Upsilon-prime and Upsilon resonances*, PhD thesis, Institute of Nuclear Physics, Krakow, 1986, DESY-F31-86-02.
- [70] LHCb collaboration, R. Aaij *et al.*, *Measurement of b-hadron masses*, Phys. Lett. **B708** (2012) 241, arXiv:1112.4896.
- [71] LHCb collaboration, R. Aaij *et al.*, *Precision measurement of D meson mass differences*, JHEP **06** (2013) 065, arXiv:1304.6865.

LHCb collaboration

R. Aaij⁴⁰, B. Adeva³⁹, M. Adinolfi⁴⁸, Z. Ajaltouni⁵, S. Akar⁵⁹, J. Albrecht¹⁰, F. Alessio⁴⁰, M. Alexander⁵³, A. Alfonso Alberio³⁸, S. Ali⁴³, G. Alkhazov³¹, P. Alvarez Cartelle⁵⁵, A.A. Alves Jr⁵⁹, S. Amato², S. Amerio²³, Y. Amhis⁷, L. An³, L. Anderlini¹⁸, G. Andreassi⁴¹, M. Andreotti^{17,g}, J.E. Andrews⁶⁰, R.B. Appleby⁵⁶, F. Archilli⁴³, P. d'Argent¹², J. Arnau Romeu⁶, A. Artamonov³⁷, M. Artuso⁶¹, E. Aslanides⁶, G. Auriemma²⁶, M. Baalouch⁵, I. Babuschkin⁵⁶, S. Bachmann¹², J.J. Back⁵⁰, A. Badalov³⁸, C. Baesso⁶², S. Baker⁵⁵, V. Balagura^{7,c}, W. Baldini¹⁷, A. Baranov³⁵, R.J. Barlow⁵⁶, C. Barschel⁴⁰, S. Barsuk⁷, W. Barter⁵⁶, F. Baryshnikov³², V. Batozskaya²⁹, V. Battista⁴¹, A. Bay⁴¹, L. Beaucourt⁴, J. Beddow⁵³, F. Bedeschi²⁴, I. Bediaga¹, A. Beiter⁶¹, L.J. Bel⁴³, N. Bely⁶³, V. Bellec⁴¹, N. Belloli^{21,i}, K. Belous³⁷, I. Belyaev³², E. Ben-Haim⁸, G. Bencivenni¹⁹, S. Benson⁴³, S. Beranek⁹, A. Berezhnoy³³, R. Bernet⁴², D. Berninghoff¹², E. Bertholet⁸, A. Bertolin²³, C. Betancourt⁴², F. Betti¹⁵, M.-O. Bettler⁴⁰, M. van Beuzekom⁴³, I.a. Bezshyiko⁴², S. Bifani⁴⁷, P. Billoir⁸, A. Birnkraut¹⁰, A. Bitadze⁵⁶, A. Bizzeti^{18,u}, M.B. Bjoern⁵⁷, T. Blake⁵⁰, F. Blanc⁴¹, J. Blouw^{11,†}, S. Blusk⁶¹, V. Bocci²⁶, T. Boettcher⁵⁸, A. Bondar^{36,w}, N. Bondar³¹, W. Bonivento¹⁶, I. Bordyuzhin³², A. Borgheresi^{21,i}, S. Borghi⁵⁶, M. Borisyak³⁵, M. Borsato³⁹, M. Borysova⁴⁶, F. Bossu⁷, M. Boubdir⁹, T.J.V. Bowcock⁵⁴, E. Bowen⁴², C. Bozzi^{17,40}, S. Braun¹², T. Britton⁶¹, J. Brodzicka²⁷, D. Brundu¹⁶, E. Buchanan⁴⁸, C. Burr⁵⁶, A. Bursche^{16,f}, J. Buytaert⁴⁰, W. Byczynski⁴⁰, S. Cadeddu¹⁶, H. Cai⁶⁴, R. Calabrese^{17,g}, R. Calladine⁴⁷, M. Calvi^{21,i}, M. Calvo Gomez^{38,m}, A. Camboni³⁸, P. Campana¹⁹, D.H. Campora Perez⁴⁰, L. Capriotti⁵⁶, A. Carbone^{15,e}, G. Carboni^{25,j}, R. Cardinale^{20,h}, A. Cardini¹⁶, P. Carniti^{21,i}, L. Carson⁵², K. Carvalho Akiba², G. Casse⁵⁴, L. Cassina^{21,i}, L. Castillo Garcia⁴¹, M. Cattaneo⁴⁰, G. Cavallero^{20,40,h}, R. Cenci^{24,t}, D. Chamont⁷, M. Charles⁸, Ph. Charpentier⁴⁰, G. Chatzikonstantinidis⁴⁷, M. Chefdeville⁴, S. Chen⁵⁶, S.F. Cheung⁵⁷, S.-G. Chitic⁴⁰, V. Chobanova³⁹, M. Chruszcz^{42,27}, A. Chubykin³¹, P. Ciambrone¹⁹, X. Cid Vidal³⁹, G. Ciezarek⁴³, P.E.L. Clarke⁵², M. Clemencic⁴⁰, H.V. Cliff⁴⁹, J. Closier⁴⁰, J. Cogan⁶, E. Cogneras⁵, V. Cogoni^{16,f}, L. Cojocariu³⁰, P. Collins⁴⁰, T. Colombo⁴⁰, A. Comerma-Montells¹², A. Contu⁴⁰, A. Cook⁴⁸, G. Coombs⁴⁰, S. Coquereau³⁸, G. Corti⁴⁰, M. Corvo^{17,g}, C.M. Costa Sobral⁵⁰, B. Couturier⁴⁰, G.A. Cowan⁵², D.C. Craik⁵⁸, A. Crocombe⁵⁰, M. Cruz Torres⁶², R. Currie⁵², C. D'Ambrosio⁴⁰, F. Da Cunha Marinho², E. Dall'Occo⁴³, J. Dalseno⁴⁸, A. Davis³, O. De Aguiar Francisco⁵⁴, S. De Capua⁵⁶, M. De Cian¹², J.M. De Miranda¹, L. De Paula², M. De Serio^{14,d}, P. De Simone¹⁹, C.T. Dean⁵³, D. Decamp⁴, L. Del Buono⁸, H.-P. Dembinski¹¹, M. Demmer¹⁰, A. Dendek²⁸, D. Derkach³⁵, O. Deschamps⁵, F. Dettori⁵⁴, B. Dey⁶⁵, A. Di Canto⁴⁰, P. Di Nezza¹⁹, H. Dijkstra⁴⁰, F. Dordei⁴⁰, M. Dorigo⁴¹, A. Dosil Suárez³⁹, L. Douglas⁵³, A. Dovbnya⁴⁵, K. Dreimanis⁵⁴, L. Dufour⁴³, G. Dujany⁸, P. Durante⁴⁰, R. Dzhelyadin³⁷, M. Dziwiecki¹², A. Dziurda⁴⁰, A. Dzyuba³¹, S. Easo⁵¹, M. Ebert⁵², U. Egede⁵⁵, V. Egorychev³², S. Eidelman^{36,w}, S. Eisenhardt⁵², U. Eitschberger¹⁰, R. Ekelhof¹⁰, L. Eklund⁵³, S. Ely⁶¹, S. Esen¹², H.M. Evans⁴⁹, T. Evans⁵⁷, A. Falabella¹⁵, N. Farley⁴⁷, S. Farry⁵⁴, R. Fay⁵⁴, D. Fazzini^{21,i}, L. Federici²⁵, D. Ferguson⁵², G. Fernandez³⁸, P. Fernandez Declara⁴⁰, A. Fernandez Prieto³⁹, F. Ferrari¹⁵, F. Ferreira Rodrigues², M. Ferro-Luzzi⁴⁰, S. Filippov³⁴, R.A. Fini¹⁴, M. Fiore^{17,g}, M. Fiorini^{17,g}, M. Firlej²⁸, C. Fitzpatrick⁴¹, T. Fiutowski²⁸, F. Fleuret^{7,b}, K. Fohl⁴⁰, M. Fontana^{16,40}, F. Fontanelli^{20,h}, D.C. Forshaw⁶¹, R. Forty⁴⁰, V. Franco Lima⁵⁴, M. Frank⁴⁰, C. Frei⁴⁰, J. Fu^{22,q}, W. Funk⁴⁰, E. Furfaro^{25,j}, C. Färber⁴⁰, E. Gabriel⁵², A. Gallas Torreira³⁹, D. Galli^{15,e}, S. Gallorini²³, S. Gambetta⁵², M. Gandelman², P. Gandini⁵⁷, Y. Gao³, L.M. Garcia Martin⁷⁰, J. García Pardiñas³⁹, J. Garra Tico⁴⁹, L. Garrido³⁸, P.J. Garsed⁴⁹, D. Gascon³⁸, C. Gaspar⁴⁰, L. Gavardi¹⁰, G. Gazzoni⁵, D. Gerick¹², E. Gersabeck¹², M. Gersabeck⁵⁶, T. Gershon⁵⁰, Ph. Ghez⁴, S. Gianì⁴¹, V. Gibson⁴⁹, O.G. Girard⁴¹, L. Giubega³⁰, K. Gizdov⁵², V.V. Gligorov⁸, D. Golubkov³², A. Golutvin^{55,40}, A. Gomes^{1,a},

I.V. Gorelov³³, C. Gotti^{21,i}, E. Govorkova⁴³, J.P. Grabowski¹², R. Graciani Diaz³⁸,
 L.A. Granado Cardoso⁴⁰, E. Graugés³⁸, E. Graverini⁴², G. Graziani¹⁸, A. Grecu³⁰, R. Greim⁹,
 P. Griffith¹⁶, L. Grillo^{21,40,i}, L. Gruber⁴⁰, B.R. Gruberg Cazon⁵⁷, O. Grünberg⁶⁷, E. Gushchin³⁴,
 Yu. Guz³⁷, T. Gys⁴⁰, C. Göbel⁶², T. Hadavizadeh⁵⁷, C. Hadjivasiliou⁵, G. Haefeli⁴¹, C. Haen⁴⁰,
 S.C. Haines⁴⁹, B. Hamilton⁶⁰, X. Han¹², T. Hancock⁵⁷, S. Hansmann-Menzemer¹², N. Harnew⁵⁷,
 S.T. Harnew⁴⁸, J. Harrison⁵⁶, C. Hasse⁴⁰, M. Hatch⁴⁰, J. He⁶³, M. Hecker⁵⁵, K. Heinicke¹⁰,
 A. Heister⁹, K. Hennessy⁵⁴, P. Henrard⁵, L. Henry⁷⁰, E. van Herwijnen⁴⁰, M. Heß⁶⁷,
 A. Hicheur², D. Hill⁵⁷, C. Hombach⁵⁶, P.H. Hopchev⁴¹, Z.-C. Huard⁵⁹, W. Hulsbergen⁴³,
 T. Humair⁵⁵, M. Hushchyn³⁵, D. Hutchcroft⁵⁴, P. Ibis¹⁰, M. Idzik²⁸, P. Ilten⁵⁸, R. Jacobsson⁴⁰,
 J. Jalocha⁵⁷, E. Jans⁴³, A. Jawahery⁶⁰, F. Jiang³, M. John⁵⁷, D. Johnson⁴⁰, C.R. Jones⁴⁹,
 C. Joram⁴⁰, B. Jost⁴⁰, N. Jurik⁵⁷, S. Kandybei⁴⁵, M. Karacson⁴⁰, J.M. Kariuki⁴⁸, S. Karodia⁵³,
 N. Kazeev³⁵, M. Kecke¹², M. Kelsey⁶¹, M. Kenzie⁴⁹, T. Ketel⁴⁴, E. Khairullin³⁵, B. Khanji¹²,
 C. Khurewathanakul⁴¹, T. Kirn⁹, S. Klaver⁵⁶, K. Klimaszewski²⁹, T. Klimovich¹¹, S. Koliiev⁴⁶,
 M. Kolpin¹², I. Komarov⁴¹, R. Kopečna¹², P. Koppenburg⁴³, A. Kosmyntseva³²,
 S. Kotriakhova³¹, M. Kozeiha⁵, M. Kreps⁵⁰, P. Krokovny^{36,w}, F. Kruse¹⁰, W. Krzemien²⁹,
 W. Kucewicz^{27,l}, M. Kucharczyk²⁷, V. Kudryavtsev^{36,w}, A.K. Kuonen⁴¹, K. Kurek²⁹,
 T. Kvaratskheliya^{32,40}, D. Lacarrere⁴⁰, G. Lafferty⁵⁶, A. Lai¹⁶, G. Lanfranchi¹⁹,
 C. Langenbruch⁹, T. Latham⁵⁰, C. Lazzeroni⁴⁷, R. Le Gac⁶, J. van Leerdam⁴³, A. Leflat^{33,40},
 J. Lefrançois⁷, R. Lefèvre⁵, F. Lemaitre⁴⁰, E. Lemos Cid³⁹, O. Leroy⁶, T. Lesiak²⁷,
 B. Leverington¹², P.-R. Li⁶³, T. Li³, Y. Li⁷, Z. Li⁶¹, T. Likhomanenko⁶⁸, R. Lindner⁴⁰,
 F. Lionetto⁴², V. Lisovskyi⁷, X. Liu³, D. Loh⁵⁰, A. Loi¹⁶, I. Longstaff⁵³, J.H. Lopes²,
 D. Lucchesi^{23,o}, M. Lucio Martinez³⁹, H. Luo⁵², A. Lupato²³, E. Luppi^{17,g}, O. Lupton⁴⁰,
 A. Lusiani²⁴, X. Lyu⁶³, F. Machefert⁷, F. Maciuc³⁰, V. Macko⁴¹, P. Mackowiak¹⁰, B. Maddock⁵⁹,
 S. Maddrell-Mander⁴⁸, O. Maev³¹, K. Maguire⁵⁶, D. Maisuzenko³¹, M.W. Majewski²⁸,
 S. Malde⁵⁷, A. Malinin⁶⁸, T. Maltsev³⁶, G. Manca^{16,f}, G. Mancinelli⁶, P. Manning⁶¹,
 D. Marangotto^{22,q}, J. Maratas^{5,v}, J.F. Marchand⁴, U. Marconi¹⁵, C. Marin Benito³⁸,
 M. Marinangeli⁴¹, P. Marino⁴¹, J. Marks¹², G. Martellotti²⁶, M. Martin⁶, M. Martinelli⁴¹,
 D. Martinez Santos³⁹, F. Martinez Vidal⁷⁰, D. Martins Tostes², L.M. Massacrier⁷,
 A. Massafferri¹, R. Matev⁴⁰, A. Mathad⁵⁰, Z. Mathe⁴⁰, C. Matteuzzi²¹, A. Mauri⁴²,
 E. Maurice^{7,b}, B. Maurin⁴¹, A. Mazurov⁴⁷, M. McCann^{55,40}, A. McNab⁵⁶, R. McNulty¹³,
 J.V. Mead⁵⁴, B. Meadows⁵⁹, C. Meaux⁶, F. Meier¹⁰, N. Meinert⁶⁷, D. Melnychuk²⁹, M. Merk⁴³,
 A. Merli^{22,40,q}, E. Michielin²³, D.A. Milanese⁶⁶, E. Millard⁵⁰, M.-N. Minard⁴, L. Minzoni¹⁷,
 D.S. Mitzel¹², A. Mogini⁸, J. Molina Rodriguez¹, T. Mombacher¹⁰, I.A. Monroy⁶⁶, S. Monteil⁵,
 M. Morandin²³, M.J. Morello^{24,t}, O. Morgunova⁶⁸, J. Moron²⁸, A.B. Morris⁵², R. Mountain⁶¹,
 F. Muheim⁵², M. Mulder⁴³, D. Müller⁵⁶, J. Müller¹⁰, K. Müller⁴², V. Müller¹⁰, P. Naik⁴⁸,
 T. Nakada⁴¹, R. Nandakumar⁵¹, A. Nandi⁵⁷, I. Nasteva², M. Needham⁵², N. Neri^{22,40},
 S. Neubert¹², N. Neufeld⁴⁰, M. Neuner¹², T.D. Nguyen⁴¹, C. Nguyen-Mau^{41,n}, S. Nieswand⁹,
 R. Niet¹⁰, N. Nikitin³³, T. Nikodem¹², A. Nogay⁶⁸, D.P. O’Hanlon⁵⁰, A. Oblakowska-Mucha²⁸,
 V. Obraztsov³⁷, S. Ogilvy¹⁹, R. Oldeman^{16,f}, C.J.G. Onderwater⁷¹, A. Ossowska²⁷,
 J.M. Otalora Goicochea², P. Owen⁴², A. Oyanguren⁷⁰, P.R. Pais⁴¹, A. Palano^{14,d},
 M. Palutan^{19,40}, A. Papanestis⁵¹, M. Pappagallo^{14,d}, L.L. Pappalardo^{17,g}, C. Pappenheimer⁵⁹,
 W. Parker⁶⁰, C. Parkes⁵⁶, G. Passaleva¹⁸, A. Pastore^{14,d}, M. Patel⁵⁵, C. Patrignani^{15,e},
 A. Pearce⁴⁰, A. Pellegrino⁴³, G. Penso²⁶, M. Pepe Altarelli⁴⁰, S. Perazzini⁴⁰, P. Perret⁵,
 L. Pescatore⁴¹, K. Petridis⁴⁸, A. Petrolini^{20,h}, A. Petrov⁶⁸, M. Petruzzo^{22,q},
 E. Picatoste Olloqui³⁸, B. Pietrzyk⁴, M. Pikiés²⁷, D. Pinci²⁶, A. Pistone^{20,h}, A. Piucci¹²,
 V. Placinta³⁰, S. Playfer⁵², M. Plo Casasus³⁹, F. Polci⁸, M. Poli Lener¹⁹, A. Poluektov^{50,36},
 I. Polyakov⁶¹, E. Polycarpo², G.J. Pomery⁴⁸, S. Ponce⁴⁰, A. Popov³⁷, D. Popov^{11,40},
 S. Poslavskii³⁷, C. Potterat², E. Price⁴⁸, J. Prisciandaro³⁹, C. Prouve⁴⁸, V. Pugatch⁴⁶,
 A. Puig Navarro⁴², H. Pullen⁵⁷, G. Punzi^{24,p}, W. Qian⁵⁰, R. Quagliani^{7,48}, B. Quintana⁵,
 B. Rachwal²⁸, J.H. Rademacker⁴⁸, M. Rama²⁴, M. Ramos Pernas³⁹, M.S. Rangel², I. Raniuk^{45,†},

F. Ratnikov³⁵, G. Raven⁴⁴, M. Ravonel Salzgeber⁴⁰, M. Reboud⁴, F. Redi⁵⁵, S. Reichert¹⁰, A.C. dos Reis¹, C. Remon Alepuz⁷⁰, V. Renaudin⁷, S. Ricciardi⁵¹, S. Richards⁴⁸, M. Rihl⁴⁰, K. Rinnert⁵⁴, V. Rives Molina³⁸, P. Robbe⁷, A. Robert⁸, A.B. Rodrigues¹, E. Rodrigues⁵⁹, J.A. Rodriguez Lopez⁶⁶, P. Rodriguez Perez^{56,†}, A. Rogozhnikov³⁵, S. Roiser⁴⁰, A. Rollings⁵⁷, V. Romanovskiy³⁷, A. Romero Vidal³⁹, J.W. Ronayne¹³, M. Rotondo¹⁹, M.S. Rudolph⁶¹, T. Ruf⁴⁰, P. Ruiz Valls⁷⁰, J. Ruiz Vidal⁷⁰, J.J. Saborido Silva³⁹, E. Sadykhov³², N. Sagidova³¹, B. Saitta^{16,f}, V. Salustino Guimaraes¹, D. Sanchez Gonzalo³⁸, C. Sanchez Mayordomo⁷⁰, B. Sanmartin Sedes³⁹, R. Santacesaria²⁶, C. Santamarina Rios³⁹, M. Santimaria¹⁹, E. Santovetti^{25,j}, G. Sarpis⁵⁶, A. Sarti²⁶, C. Satriano^{26,s}, A. Satta²⁵, D.M. Saunders⁴⁸, D. Savrina^{32,33}, S. Schael⁹, M. Schellenberg¹⁰, M. Schiller⁵³, H. Schindler⁴⁰, M. Schlupp¹⁰, M. Schmelling¹¹, T. Schmelzer¹⁰, B. Schmidt⁴⁰, O. Schneider⁴¹, A. Schopper⁴⁰, H.F. Schreiner⁵⁹, K. Schubert¹⁰, M. Schubiger⁴¹, M.-H. Schune⁷, R. Schwemmer⁴⁰, B. Sciascia¹⁹, A. Sciubba^{26,k}, A. Semennikov³², A. Sergi⁴⁷, N. Serra⁴², J. Serrano⁶, L. Sestini²³, P. Seyfert⁴⁰, M. Shapkin³⁷, I. Shapoval⁴⁵, Y. Shcheglov³¹, T. Shears⁵⁴, L. Shekhtman^{36,w}, V. Shevchenko⁶⁸, B.G. Siddi^{17,40}, R. Silva Coutinho⁴², L. Silva de Oliveira², G. Simi^{23,o}, S. Simone^{14,d}, M. Sirendi⁴⁹, N. Skidmore⁴⁸, T. Skwarnicki⁶¹, E. Smith⁵⁵, I.T. Smith⁵², J. Smith⁴⁹, M. Smith⁵⁵, I. Soares Lavra¹, M.D. Sokoloff⁵⁹, F.J.P. Soler⁵³, B. Souza De Paula², B. Spaan¹⁰, P. Spradlin⁵³, S. Sridharan⁴⁰, F. Stagni⁴⁰, M. Stahl¹², S. Stahl⁴⁰, P. Stefko⁴¹, S. Stefkova⁵⁵, O. Steinkamp⁴², S. Stemmler¹², O. Stenyakin³⁷, M. Stepanova³¹, H. Stevens¹⁰, S. Stone⁶¹, B. Storaci⁴², S. Stracka^{24,p}, M.E. Stramaglia⁴¹, M. Straticiu³⁰, U. Straumann⁴², L. Sun⁶⁴, W. Sutcliffe⁵⁵, K. Swientek²⁸, V. Syropoulos⁴⁴, M. Szczekowski²⁹, T. Szumlak²⁸, M. Szymanski⁶³, S. T’Jampens⁴, A. Tayduganov⁶, T. Tekampe¹⁰, G. Tellarini^{17,g}, F. Teubert⁴⁰, E. Thomas⁴⁰, J. van Tilburg⁴³, M.J. Tilley⁵⁵, V. Tisserand⁴, M. Tobin⁴¹, S. Tolk⁴⁹, L. Tomassetti^{17,g}, D. Tonelli²⁴, F. Toriello⁶¹, R. Tourinho Jadallah Aoude¹, E. Tournefier⁴, M. Traill⁵³, M.T. Tran⁴¹, M. Tresch⁴², A. Trisovic⁴⁰, A. Tsaregorodtsev⁶, P. Tsopelas⁴³, A. Tully⁴⁹, N. Tuning⁴³, A. Ukleja²⁹, A. Usachov⁷, A. Ustyuzhanin³⁵, U. Uwer¹², C. Vacca^{16,f}, A. Vagner⁶⁹, V. Vagnoni^{15,40}, A. Valassi⁴⁰, S. Valat⁴⁰, G. Valenti¹⁵, R. Vazquez Gomez¹⁹, P. Vazquez Regueiro³⁹, S. Vecchi¹⁷, M. van Veghel⁴³, J.J. Velthuis⁴⁸, M. Veltri^{18,r}, G. Veneziano⁵⁷, A. Venkateswaran⁶¹, T.A. Verlage⁹, M. Vernet⁵, M. Vesterinen⁵⁷, J.V. Viana Barbosa⁴⁰, B. Viaud⁷, D. Vieira⁶³, M. Vieites Diaz³⁹, H. Viemann⁶⁷, X. Vilasis-Cardona^{38,m}, M. Vitti⁴⁹, V. Volkov³³, A. Vollhardt⁴², B. Voneki⁴⁰, A. Vorobyev³¹, V. Vorobyev^{36,w}, C. Vob⁹, J.A. de Vries⁴³, C. Vázquez Sierra³⁹, R. Waldi⁶⁷, C. Wallace⁵⁰, R. Wallace¹³, J. Walsh²⁴, J. Wang⁶¹, D.R. Ward⁴⁹, H.M. Wark⁵⁴, N.K. Watson⁴⁷, D. Websdale⁵⁵, A. Weiden⁴², M. Whitehead⁴⁰, J. Wicht⁵⁰, G. Wilkinson^{57,40}, M. Wilkinson⁶¹, M. Williams⁵⁶, M.P. Williams⁴⁷, M. Williams⁵⁸, T. Williams⁴⁷, F.F. Wilson⁵¹, J. Wimberley⁶⁰, M.A. Winn⁷, J. Wishahi¹⁰, W. Wislicki²⁹, M. Witek²⁷, G. Wormser⁷, S.A. Wotton⁴⁹, K. Wraight⁵³, K. Wyllie⁴⁰, Y. Xie⁶⁵, Z. Xu⁴, Z. Yang³, Z. Yang⁶⁰, Y. Yao⁶¹, H. Yin⁶⁵, J. Yu⁶⁵, X. Yuan⁶¹, O. Yushchenko³⁷, K.A. Zarebski⁴⁷, M. Zavertyaev^{11,c}, L. Zhang³, Y. Zhang⁷, A. Zhelezov¹², Y. Zheng⁶³, X. Zhu³, V. Zhukov³³, J.B. Zonneveld⁵², S. Zucchelli¹⁵.

¹Centro Brasileiro de Pesquisas Físicas (CBPF), Rio de Janeiro, Brazil

²Universidade Federal do Rio de Janeiro (UFRJ), Rio de Janeiro, Brazil

³Center for High Energy Physics, Tsinghua University, Beijing, China

⁴LAPP, Université Savoie Mont-Blanc, CNRS/IN2P3, Annecy-Le-Vieux, France

⁵Clermont Université, Université Blaise Pascal, CNRS/IN2P3, LPC, Clermont-Ferrand, France

⁶CPPM, Aix-Marseille Université, CNRS/IN2P3, Marseille, France

⁷LAL, Université Paris-Sud, CNRS/IN2P3, Orsay, France

⁸LPNHE, Université Pierre et Marie Curie, Université Paris Diderot, CNRS/IN2P3, Paris, France

⁹I. Physikalisches Institut, RWTH Aachen University, Aachen, Germany

¹⁰Fakultät Physik, Technische Universität Dortmund, Dortmund, Germany

¹¹Max-Planck-Institut für Kernphysik (MPIK), Heidelberg, Germany

¹²Physikalisches Institut, Ruprecht-Karls-Universität Heidelberg, Heidelberg, Germany

- ¹³*School of Physics, University College Dublin, Dublin, Ireland*
- ¹⁴*Sezione INFN di Bari, Bari, Italy*
- ¹⁵*Sezione INFN di Bologna, Bologna, Italy*
- ¹⁶*Sezione INFN di Cagliari, Cagliari, Italy*
- ¹⁷*Universita e INFN, Ferrara, Ferrara, Italy*
- ¹⁸*Sezione INFN di Firenze, Firenze, Italy*
- ¹⁹*Laboratori Nazionali dell'INFN di Frascati, Frascati, Italy*
- ²⁰*Sezione INFN di Genova, Genova, Italy*
- ²¹*Universita e INFN, Milano-Bicocca, Milano, Italy*
- ²²*Sezione di Milano, Milano, Italy*
- ²³*Sezione INFN di Padova, Padova, Italy*
- ²⁴*Sezione INFN di Pisa, Pisa, Italy*
- ²⁵*Sezione INFN di Roma Tor Vergata, Roma, Italy*
- ²⁶*Sezione INFN di Roma La Sapienza, Roma, Italy*
- ²⁷*Henryk Niewodniczanski Institute of Nuclear Physics Polish Academy of Sciences, Kraków, Poland*
- ²⁸*AGH - University of Science and Technology, Faculty of Physics and Applied Computer Science, Kraków, Poland*
- ²⁹*National Center for Nuclear Research (NCBJ), Warsaw, Poland*
- ³⁰*Horia Hulubei National Institute of Physics and Nuclear Engineering, Bucharest-Magurele, Romania*
- ³¹*Petersburg Nuclear Physics Institute (PNPI), Gatchina, Russia*
- ³²*Institute of Theoretical and Experimental Physics (ITEP), Moscow, Russia*
- ³³*Institute of Nuclear Physics, Moscow State University (SINP MSU), Moscow, Russia*
- ³⁴*Institute for Nuclear Research of the Russian Academy of Sciences (INR RAN), Moscow, Russia*
- ³⁵*Yandex School of Data Analysis, Moscow, Russia*
- ³⁶*Budker Institute of Nuclear Physics (SB RAS), Novosibirsk, Russia*
- ³⁷*Institute for High Energy Physics (IHEP), Protvino, Russia*
- ³⁸*ICCUB, Universitat de Barcelona, Barcelona, Spain*
- ³⁹*Universidad de Santiago de Compostela, Santiago de Compostela, Spain*
- ⁴⁰*European Organization for Nuclear Research (CERN), Geneva, Switzerland*
- ⁴¹*Institute of Physics, Ecole Polytechnique Fédérale de Lausanne (EPFL), Lausanne, Switzerland*
- ⁴²*Physik-Institut, Universität Zürich, Zürich, Switzerland*
- ⁴³*Nikhef National Institute for Subatomic Physics, Amsterdam, The Netherlands*
- ⁴⁴*Nikhef National Institute for Subatomic Physics and VU University Amsterdam, Amsterdam, The Netherlands*
- ⁴⁵*NSC Kharkiv Institute of Physics and Technology (NSC KIPT), Kharkiv, Ukraine*
- ⁴⁶*Institute for Nuclear Research of the National Academy of Sciences (KINR), Kyiv, Ukraine*
- ⁴⁷*University of Birmingham, Birmingham, United Kingdom*
- ⁴⁸*H.H. Wills Physics Laboratory, University of Bristol, Bristol, United Kingdom*
- ⁴⁹*Cavendish Laboratory, University of Cambridge, Cambridge, United Kingdom*
- ⁵⁰*Department of Physics, University of Warwick, Coventry, United Kingdom*
- ⁵¹*STFC Rutherford Appleton Laboratory, Didcot, United Kingdom*
- ⁵²*School of Physics and Astronomy, University of Edinburgh, Edinburgh, United Kingdom*
- ⁵³*School of Physics and Astronomy, University of Glasgow, Glasgow, United Kingdom*
- ⁵⁴*Oliver Lodge Laboratory, University of Liverpool, Liverpool, United Kingdom*
- ⁵⁵*Imperial College London, London, United Kingdom*
- ⁵⁶*School of Physics and Astronomy, University of Manchester, Manchester, United Kingdom*
- ⁵⁷*Department of Physics, University of Oxford, Oxford, United Kingdom*
- ⁵⁸*Massachusetts Institute of Technology, Cambridge, MA, United States*
- ⁵⁹*University of Cincinnati, Cincinnati, OH, United States*
- ⁶⁰*University of Maryland, College Park, MD, United States*
- ⁶¹*Syracuse University, Syracuse, NY, United States*
- ⁶²*Pontifícia Universidade Católica do Rio de Janeiro (PUC-Rio), Rio de Janeiro, Brazil, associated to ²*
- ⁶³*University of Chinese Academy of Sciences, Beijing, China, associated to ³*
- ⁶⁴*School of Physics and Technology, Wuhan University, Wuhan, China, associated to ³*
- ⁶⁵*Institute of Particle Physics, Central China Normal University, Wuhan, Hubei, China, associated to ³*
- ⁶⁶*Departamento de Física, Universidad Nacional de Colombia, Bogota, Colombia, associated to ⁸*

- ⁶⁷ *Institut für Physik, Universität Rostock, Rostock, Germany, associated to* ¹²
⁶⁸ *National Research Centre Kurchatov Institute, Moscow, Russia, associated to* ³²
⁶⁹ *National Research Tomsk Polytechnic University, Tomsk, Russia, associated to* ³²
⁷⁰ *Instituto de Fisica Corpuscular, Centro Mixto Universidad de Valencia - CSIC, Valencia, Spain, associated to* ³⁸
⁷¹ *Van Swinderen Institute, University of Groningen, Groningen, The Netherlands, associated to* ⁴³

- ^a *Universidade Federal do Triângulo Mineiro (UFTM), Uberaba-MG, Brazil*
^b *Laboratoire Leprince-Ringuet, Palaiseau, France*
^c *P.N. Lebedev Physical Institute, Russian Academy of Science (LPI RAS), Moscow, Russia*
^d *Università di Bari, Bari, Italy*
^e *Università di Bologna, Bologna, Italy*
^f *Università di Cagliari, Cagliari, Italy*
^g *Università di Ferrara, Ferrara, Italy*
^h *Università di Genova, Genova, Italy*
ⁱ *Università di Milano Bicocca, Milano, Italy*
^j *Università di Roma Tor Vergata, Roma, Italy*
^k *Università di Roma La Sapienza, Roma, Italy*
^l *AGH - University of Science and Technology, Faculty of Computer Science, Electronics and Telecommunications, Kraków, Poland*
^m *LIFAELS, La Salle, Universitat Ramon Llull, Barcelona, Spain*
ⁿ *Hanoi University of Science, Hanoi, Viet Nam*
^o *Università di Padova, Padova, Italy*
^p *Università di Pisa, Pisa, Italy*
^q *Università degli Studi di Milano, Milano, Italy*
^r *Università di Urbino, Urbino, Italy*
^s *Università della Basilicata, Potenza, Italy*
^t *Scuola Normale Superiore, Pisa, Italy*
^u *Università di Modena e Reggio Emilia, Modena, Italy*
^v *Iligan Institute of Technology (IIT), Iligan, Philippines*
^w *Novosibirsk State University, Novosibirsk, Russia*
[†] *Deceased*